



Publication Year	2017
Acceptance in OA @INAF	2020-07-24T09:48:37Z
Title	High-performance cryogenic fractal 180° hybrid power divider with integrated directional coupler
Authors	LADU, Adelaide; MONTISCI, GIORGIO; VALENTE, Giuseppe; NAVARRINI, Alessandro; MARONGIU, Pasqualino; et al.
DOI	10.1002/2017RS006292
Handle	http://hdl.handle.net/20.500.12386/26615
Journal	RADIO SCIENCE
Number	52



RESEARCH ARTICLE

10.1002/2017RS006292

Special Section:

URSI General Assembly and Scientific Symposium (2017)

Key Points:

- Design of a fractal 180° hybrid power divider for the P-band cryogenic receiver of the Sardinia Radio Telescope
- Compact hybrid power divider with improved bandwidth compared to other solutions available in the literature
- Directional coupler with weak coupling and high isolation, used to calibrate the receiver, cascaded to the 180° hybrid in the same layout

Correspondence to:

G. Montisci,
giorgio.montisci@unica.it

Citation:

Ladu, A., G. Montisci, G. Valente, A. Navarrini, P. Marongiu, T. Pisanu, and G. Mazzarella (2017), High-performance cryogenic fractal 180° hybrid power divider with integrated directional coupler, *Radio Sci.*, 52, doi:10.1002/2017RS006292.

Received 5 MAR 2017

Accepted 22 MAY 2017

Accepted article online 26 MAY 2017

High-performance cryogenic fractal 180° hybrid power divider with integrated directional coupler

Adelaide Ladu¹, Giorgio Montisci^{1,2} , Giuseppe Valente^{1,3}, Alessandro Navarrini¹, Pasqualino Marongiu¹, Tonino Pisanu¹, and Giuseppe Mazzarella² 

¹Osservatorio Astronomico di Cagliari, Selargius, Italy, ²Dipartimento di Ingegneria Elettrica ed Elettronica, University of Cagliari, Cagliari, Italy, ³Agenzia Spaziale Italiana, Rome, Italy

Abstract A 180° hybrid and a directional coupler to be employed in the P-band cryogenic receiver of the Sardinia Radio Telescope are proposed in this work. An in-depth study of the issues related to the use of microwave components for cryogenic radio astronomy receivers is carried out to select the best suited technology and configuration. As a result, a planar fractal 180° hybrid configuration available in the literature has been optimized aiming to increase the operating bandwidth in order to comply with the design specifications of the application at hand. A coupled line directional coupler with weak coupling and high isolation, used to calibrate the receiver chain, is cascaded to the 180° hybrid and realized in the same layout. The final device, consisting of the 180° hybrid and the directional coupler, has been manufactured and tested at the cryogenic temperature of 20 K, showing a good agreement between experimental results and predicted performance.

1. Introduction

The 180° hybrid is a key component for microwave circuits and systems. It is used to divide a RF signal into two equal amplitude and out-of-phase outputs. Several structures are available in the literature and employ different technologies and configurations, as waveguide or planar structures. Waveguide hybrids, as the magic T junction [Pozar, 2012], [Wang and Zaki, 1996] or the Y junction [Kerr, 2001], have excellent performances and low losses. On the other hand, planar hybrids are usually fabricated in microstrip or coplanar waveguide technology, as the standard rat-race hybrid [Pozar, 2012]. Although the planar configurations have a worst performance in terms of insertion loss and phase imbalance compared to waveguide structures, they allow to achieve a wider bandwidth with a smaller dimension and weight. Nevertheless, one of the main limitation of planar structures, especially at lower frequencies, is still the large surface area occupied by these components.

As a matter of fact, based on the particular application at hand, the design of a microwave system often requires to comply with different and sometimes conflicting specifications, and this means that in the design of each device of the system, some of the output parameters are constrained, and other parameters should be properly optimized. In this context, the electromagnetic parameters of interest for a 180° hybrid are the amplitude imbalance, the phase imbalance, the return loss, and the isolation. However, other aspects should be taken into account, as the reliability, the dimension, and the weight of the component.

In this paper we present a 180° hybrid and a directional coupler to be employed in a high-performance cryogenic receiver of the Sardinia Radio Telescope (SRT) [Bollini et al., 2015], operating between 300 MHz and 410 MHz (31% relative bandwidth within the P band). In particular, the orthomode transducer for the SRT P-band receiver is based on an orthomode junction (OMJ) and on two identical 180° hybrids, which are topic of this paper. The OMJ separates the RF signal from the P-band feed horn in two linear polarizations, each one split into two out-of-phase signals (four outputs), and the two 180° hybrids are used to recombine the out-of-phase signals. A directional coupler is cascaded to each of the two 180° hybrids in order to calibrate the receiver chain by injecting a noise source and a weak coherent comb signal in the RF signal. Then, the through line is connected in front of the low-noise amplifier (LNA).

In order to reduce thermal noise, the components of the radio-astronomical receivers of SRT, including the 180° hybrids and directional couplers, will be arranged inside a cryostat at the temperature of 20 K [Valente et al., 2014; Valente et al., 2015]. The design of the cryostat used for the P-band receiver of SRT is

constrained by the limited space available in the direction of the optical axis inside the focal cabin of the radio telescope, thus requiring a very compact design of all the components of the receiver chain.

It can be easily understood that the above radio astronomy application requires that the 180° hybrids and the directional couplers have very specific features. In particular, they should be very compact, due to the limited space available inside the cryostat. Moreover, the P-band receiver is mounted at about 70 m from the ground in the primary focus position of SRT, and it can be reached for maintenance only using a crane. Therefore, all the components of the receiver operating at cryogenic temperature should also be very light and reliable, since they are subjected to several refrigeration cycles and then, to high thermal stress.

As regard the electromagnetic behavior, the impedance mismatch along the receiver chain should be reduced as possible, since it causes an increase of the system noise temperature and then reduces the sensitivity of the receiver [Pozar, 2012]. Therefore, a high return loss over the operating bandwidth (>20 dB in our case) is required at the 180° hybrid input ports.

The above considerations lead to the choice of a simple planar microstrip technology for the realization of the 180° hybrids and directional couplers. A standard coupled line configuration, aimed to maximize directivity, is adopted for the directional coupler, whereas several planar compact configurations of 180° hybrid available in the literature have been tested, seeking for a good candidate to comply with the specifications of the P-band receiver. We left out from our investigation the 180° hybrids including air bridges, via holes, and/or lumped components [Okabe *et al.*, 2004; Mo *et al.*, 2007; Yang *et al.*, 2010], since they are difficult to design at cryogenic temperatures. As a matter of fact, these configurations employ different materials (for metallization, soldering, air-bridges, and via holes) and the connection between different metallic parts is not reliable when the temperature is lowered at 20 K, due to the different thermal contraction of the different materials used (copper, gold, conductive glue, and so on). We also do not consider the 180° hybrids based on the coupled line technology [as Napijalo, 2012; Simion and Bartolucci, 2014; Liu *et al.*, 2014], since, along with being quite intricate (sometimes including also air-bridges and/or via holes), they usually have higher insertion losses and are therefore not suitable to be used in high-performance radio astronomy receivers.

As a consequence, only simply and fully planar configurations have been investigated over the frequency band of interest. In particular, using Ansys HFSS we have analyzed the compact 180° hybrids proposed by Settaluri *et al.* [2000], Chuang [2005], and Eccleston [2003] and the fractal second-iteration Moore rat-race coupler (SMRRC) proposed by Ghali and Moselhy [2004], which seem particularly promising for our application. Unfortunately, from HFSS simulated results, we have found that all these solutions do not comply with the specifications of the P-band receiver, mainly for the return loss and amplitude imbalance. However, we also noticed that the SMRRC of Ghali provides a simple and very compact configuration, with the best performance in terms of amplitude imbalance over the analyzed configurations. Therefore, the latter configuration has been selected as the starting point for our design. An optimized configuration of the SMRRC is then proposed in this work. In particular, a suitable modification of the characteristic impedances of the lines between the input ports has been carried out, aiming to increase the operating bandwidth to comply with all the requirements of the P-band radio astronomy receiver. The cascaded directional coupler, with a low coupling factor and a high directivity, is integrated within the same PCB of the 180° hybrid to save space inside the cryostat.

A prototype of the complete component, including both the 180° hybrid and the directional coupler connected together, has been manufactured in the microwave laboratory of the Cagliari Astronomy Observatory and tested at 20 K, showing a very good agreement with the design specifications.

2. Design and Optimization of the Fractal 180° Hybrid Power Divider

The 180° hybrid has been designed on a substrate of Arlon AD1000 of thickness 3.2258 mm, with a dielectric permittivity of 10.9 at room temperature (300 K). The dielectric loss tangent is less than 0.0015 at 410 MHz, and the thickness of the metallization is 17 μm . A number of configurations available in the literature, simple and fully planar, and therefore best suited for implementation at cryogenic temperature, have been analyzed using Ansys HFSS, and the results are reported in Table 1. However, these hybrids do not comply with the required specifications over the operating band (300 MHz–410 MHz): they all have a high amplitude imbalance the Settaluri *et al.*'s [2000] and Chuang's [2005] configurations have low return loss; and the

Table 1. Comparison Between Different Configurations of 180° Hybrids (HFSS Simulated Results) Over the Frequency Range 300 MHz–410 MHz

	Reflection	Amplitude Imbalance	Phase Imbalance	Planar Dimension
Design Specifications	< -20 dB	0.5 dB	180° ± 10°	≤100 × 100 mm ²
Settaluri	< -15 dB	1.45 dB	180° ± 11°	115 × 110 mm ²
Chuang	< -16 dB	1.20 dB	180° ± 11°	135 × 70 mm ²
Eccleston	< -19 dB	1.20 dB	180° ± 10°	170 × 70 mm ²
Ghali	< -18 dB	1.0 dB	180° ± 11°	100 × 100 mm ²
Optimized	< -20 dB	0.5 dB	180° ± 10°	100 × 100 mm ²

Settaluri’s, Chuang’s, and Eccleston’s [2003] hybrids are also slightly too large. After all, the Ghali and Moselhy’s [2004] configuration seems the best one. Therefore, it has been selected and then optimized aiming to comply with all the specifications of the P-band radio astronomy receiver of SRT (see the first row of Table 1).

Hence, the standard SMRRC proposed by Ghali is considered as the starting point for our design. It employs 70.7 Ω microstrip lines, bended according to the Moore fractal theory of the second order. Using the selected substrate, the width of the lines is 1.17 mm. The HFSS model of this component is shown in Figure 1a.

At this point, the Ghali’s configuration needs to be improved to enhance the operating bandwidth according to the design specifications. However, the fractal hybrid is nothing but a standard rat-race hybrid with the lines meandered according to the second-iteration Moore fractal and so it has the same electromagnetic performance of the standard hybrid. Therefore, in order to reach our design goal, we first decided to investigate a strategy to improve the operating bandwidth of the standard rat-race hybrid (Figure 1b). Then, the optimized hybrid has been implemented as a fractal one, to cope with the size requirements (Table 1).

It is well known that the bandwidth of a lossless network is inversely proportional to the electromagnetic energy stored in the network itself [Foster, 1924; Fano, 1947; Nedlin, 1989]. In a transmission line circuit, the stored energy depends both on the electrical lengths of the lines and on their characteristic impedances. Since the electrical lengths of the four lines between the ports of the rat-race hybrid are constrained, we decided to modify their impedances with the goal of reducing the overall stored electromagnetic energy in order to increase the bandwidth. Then, let Z_1 be the characteristic impedance of the line between ports 3–1; Z_2 be the impedance of the lines between ports 1–2, and between ports 4–3; and Z_3 be the impedance of the line between ports 2–4 (Figure 1b). In order to find the values of Z_1 , Z_2 , and Z_3 needed to get the required bandwidth, a random optimization procedure with respect to the variables Z_1 , Z_2 , and Z_3 has been performed using Keysight Technologies Advanced Design System (ADS), based on a simple transmission line model of the hybrid (Figure 2), with the constraint that Z_1 , Z_2 , and Z_3 can lie in a range of ±10% around the theoretical value of 70.7 Ω. The goals of this optimization were a return loss larger than 20 dB at all the ports,

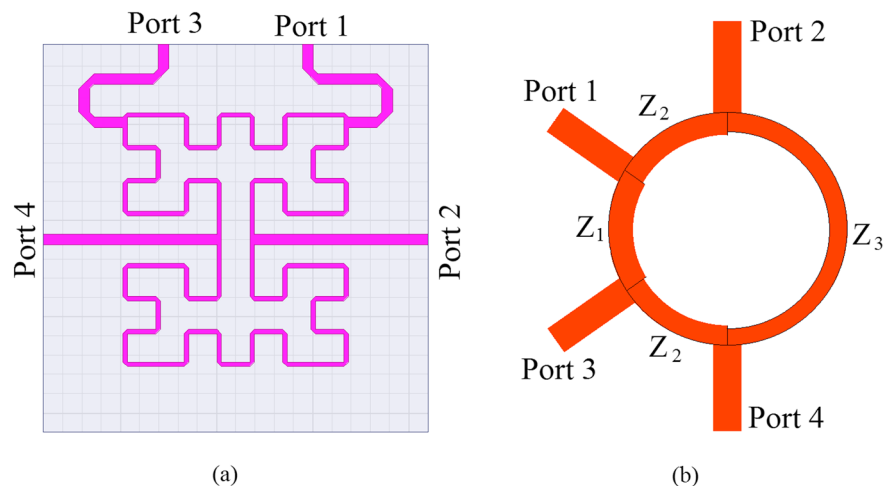


Figure 1. (a) Fractal second-iteration Moore rat-race coupler proposed by Ghali. (b) Standard rat-race hybrid with modified impedances.

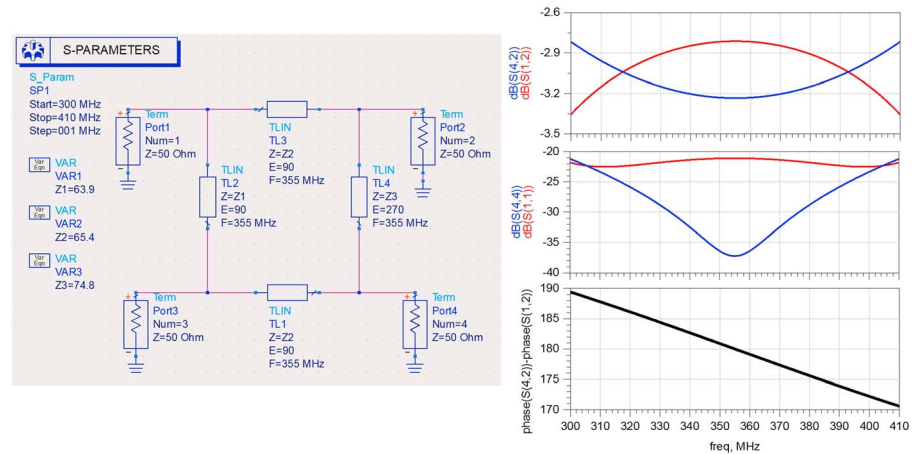
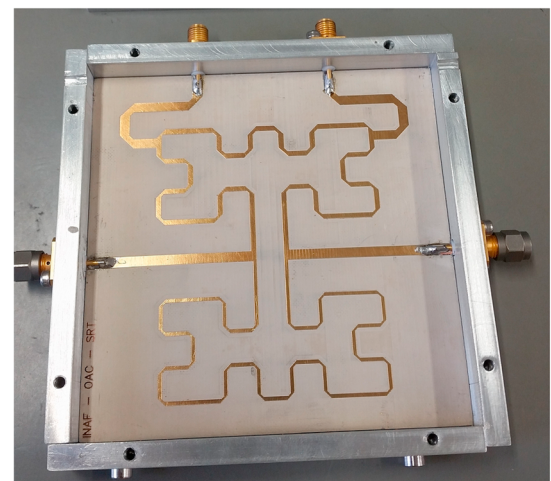
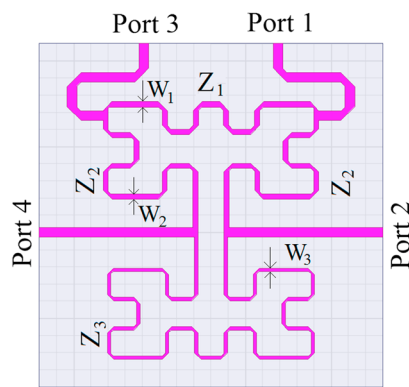


Figure 2. ADS transmission line model of the rat-race hybrid and scattering parameters of the optimized hybrid for $Z_1 = 63.9 \Omega$, $Z_2 = 65.4 \Omega$, and $Z_3 = 74.8 \Omega$.

an amplitude imbalance less than 0.5 dB, and a phase imbalance between 170° and 190° over the required bandwidth. The optimization converged to $Z_1 = 63.9 \Omega$, $Z_2 = 65.4 \Omega$, and $Z_3 = 74.8 \Omega$ and the resulting simulated (ADS) scattering parameters of the hybrid are reported in Figure 2, fulfilling the required performance.

Based on the above results, we have modified also the impedances of the four lines between the ports of the Ghali’s fractal hybrid, using the values optimized by ADS (Figure 3a). The width of the lines, their physical lengths, and all the 90° bends have been computed using the design formulas of *Wadel* [1991]. Then, the resulting structure has been simulated with Ansys HFSS to assess its performance and confirm the requested bandwidth.

The Ansys HFSS simulated results of both the standard 180° hybrid coupler (Figure 1a) and the optimized configuration (Figure 3a) are shown in Figure 4 (reflection coefficients S_{11} , S_{44} and transmission coefficients S_{21} , S_{24}), and in Figure 5 (phase imbalance for the Δ port), and are summarized in Table 1. The optimized component provides a larger bandwidth than the standard SMRRC for both the reflection coefficient (the -20 dB bandwidth improves from 28% to 34%) and the amplitude imbalance (the 0.5 dB bandwidth improves from 24% to 32%), and it satisfies all the design specifications within the operating frequency of the SRT P-band receiver (Table 1).



(a)

(b)

Figure 3. (a) HFSS model of the optimized fractal second-iteration Moore rat-race coupler ($Z_1 = 63.9 \Omega$, $Z_2 = 65.4 \Omega$, and $Z_3 = 74.8 \Omega$; $W_1 = 1.55$ mm, $W_2 = 1.46$ mm, and $W_3 = 0.99$). (b) Prototype of the optimized hybrid.

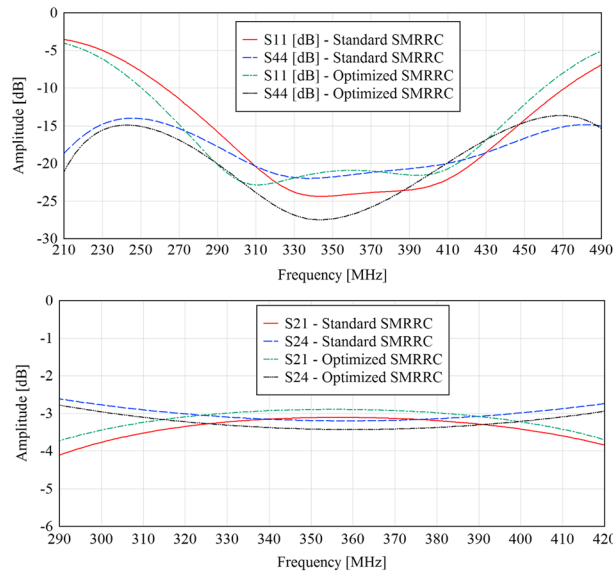


Figure 4. Simulated (HFSS) scattering parameters of the standard SMRRC and of the optimized 180° hybrid proposed in this paper.

performance, making it suitable to be employed in the P-band cryogenic receiver of the Sardinia Radio Telescope. A directional coupler has been inserted in the through line of the 180° hybrid, within the same PCB (i.e., cascaded to port 2 of the 180° hybrid), in order to inject a noise source in the RF signal (see Figure 7). The choice of embedding the 180° hybrid and the directional coupler in the same layout brings several advantages: minimizes the losses in front of the LNA (which is directly connected to output of the directional coupler), since there are no connectors or cables between the hybrid and the directional coupler; reduces the dimension occupied by these two components inside the cryostat; and reduces the production cost.

The resulting component has six ports, and it is shown in Figure 7. The two out-of-phase signals from the OMJ feed ports 1 and 4, respectively, and port 2 provide the recombined signal for the selected polarization, added to the noise signal injected from port 6. For the required application, ports 3 and 5 will be terminated in matched loads.

In section 2 we have designed the 180° hybrid power divider at room temperature (300 K). This design cannot be reused at cryogenic temperature because, at the temperature of 20 K, both the mechanical and the electrical properties of the Arlon AD1000 substrate are different. In particular, the main consequences of the temperature reduction are the modification of the dielectric permittivity and the contraction of the material. However, as a first approximation, we can assume to take into account both these effects leaving unmodified the substrate thickness, and using an “equivalent” value of the dielectric permittivity. In order to evaluate the equivalent dielectric permittivity to be used for the design at 20 K we have measured, at this temperature, the scattering parameters of a through microstrip line of fixed width and length, and, by comparison with the Ansys HFSS simulated results, we have derived an equivalent dielectric permittivity of 12.5.

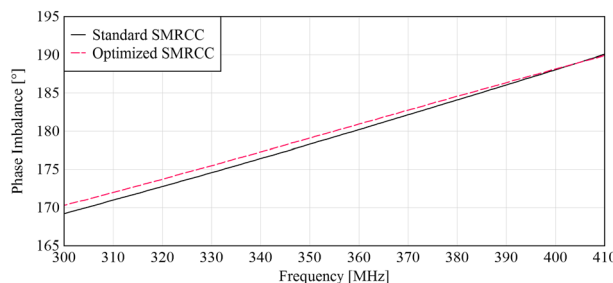


Figure 5. Simulated (HFSS) phase imbalance of the standard SMRRC and of the optimized 180° hybrid proposed in this paper.

A prototype of the optimized 180° hybrid has been realized in the laboratories of the Astronomical Observatory of Cagliari (Figure 3b) and tested at room temperature (300 K) in order to assess the improvements of the optimized hybrid over the standard SMRRC configuration. Comparisons between HFSS simulated results and measurements are shown in Figure 6, with an excellent agreement.

3. Cryogenic Design of the Fractal 180° Hybrid and Directional Coupler

The simple and fully planar fractal hybrid configuration, designed and experimentally tested in the previous section at room temperature (300 K), has a very compact size and has demonstrated an excellent electromagnetic

performance, making it suitable to be employed in the P-band cryogenic receiver of the Sardinia Radio Telescope. A directional coupler has been inserted in the through line of the 180° hybrid, within the same PCB (i.e., cascaded to port 2 of the 180° hybrid), in order to inject a noise source in the RF signal (see Figure 7). The choice of embedding the 180° hybrid and the directional coupler in the same layout brings several advantages: minimizes the losses in front of the LNA (which is directly connected to output of the directional coupler), since there are no connectors or cables between the hybrid and the directional coupler; reduces the dimension occupied by these two components inside the cryostat; and reduces the production cost.

In conclusion, the directional coupler operating at 20 K must be designed using a substrate of thickness 3.2258 mm and dielectric permittivity 12.5, whereas the 180° hybrid should be redesigned by using a dielectric permittivity of 12.5 instead of 10.9 (which is the value at 300 K). The new design of the 180° hybrid has been

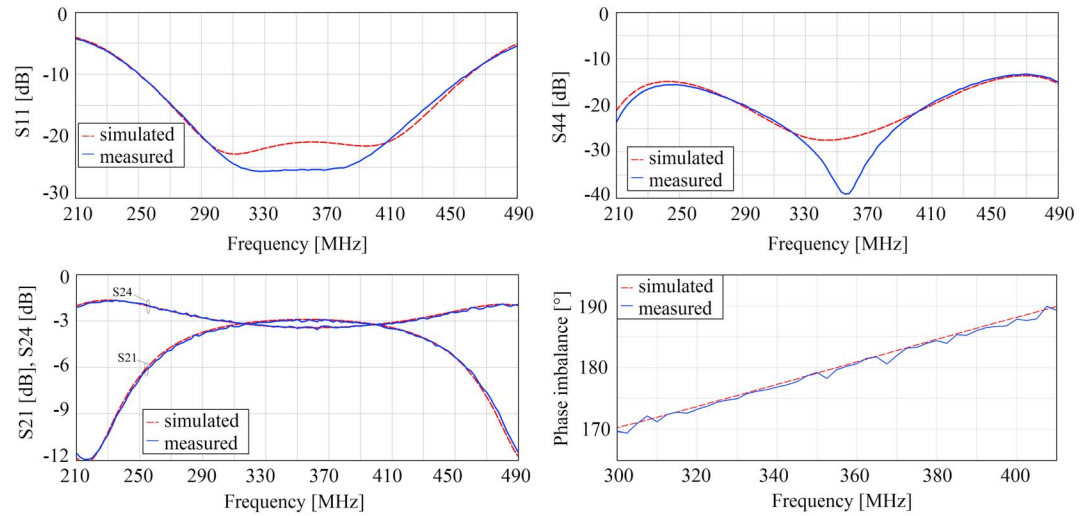


Figure 6. Simulated (HFSS) and measured frequency response of the optimized 180° hybrid in Figure 3.

performed by using the same characteristic impedances derived for the design at room temperature (namely $Z_1 = 63.9 \Omega$, $Z_2 = 65.4 \Omega$, and $Z_3 = 74.8 \Omega$), and the physical lengths of the lines have been properly scaled keeping the same electrical lengths of the initial design. The simulated results are virtually the same as provided by the design at room temperature with return loss below -20 dB, amplitude imbalance of 0.5 dB, and phase imbalance of $180^\circ \pm 10^\circ$ in the operating frequency band.

3.1. Design of the Directional Coupler

The directional coupler is used to calibrate the receiver chain by injecting a noise source and a weak coherent comb signal in the RF signal. Therefore, it should provide a weak coupling C (namely, -26 dB in our case) at the center frequency and a directivity D larger than 20 dB over the operating frequency band. This performance has been achieved by using a coupled microstrip line directional coupler with small electrical length $\vartheta < < 1$. In fact, due to the small coupling region, such a configuration does not require to compensate for the different phase velocities of the coupled line modes and provides a high isolation without the need of intricate solutions (as the addition of capacitive elements or nonplanar components) [Iwer, 1980; Kim et al., 2004; Dydyk, 1999]. The well-known design equations for a coupled line microstrip directional coupler [Poazar, 2012] can be approximated, for $\vartheta < < 1$, as

$$S_{11} \approx \frac{1}{4} j \text{sen } \vartheta \left[\left(Z_e - \frac{1}{Z_e} \right) + \left(Z_o - \frac{1}{Z_o} \right) \right] \quad (1)$$

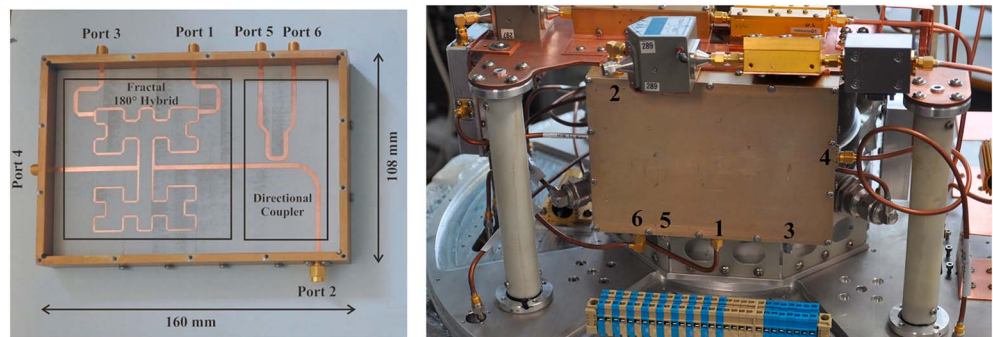


Figure 7. (left) Prototype of the fractal 180° hybrid and directional coupler and (right) photo of the component installed in the receiver.

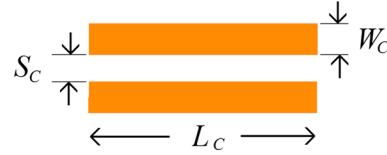


Figure 8. Geometry of standard microstrip coupled line directional coupler.

$$S_{31} \approx \frac{1}{4} j \text{sen } \vartheta \left[\left(Z_e - \frac{1}{Z_e} \right) - \left(Z_o - \frac{1}{Z_o} \right) \right] \quad (2)$$

$$S_{41} \approx \frac{1}{4} j \text{sen } \vartheta \left[\left(Z_e + \frac{1}{Z_e} \right) - \left(Z_o + \frac{1}{Z_o} \right) \right] \quad (3)$$

wherein Z_e and Z_o are the normalized even and odd characteristic impedances of the coupled line section. Now if we let $Z_e Z_o = 1 + \delta$ with $\delta \ll 1$, as required for a coupled line section with good input matching at all the ports, we obtain

$$S_{11} \approx \frac{1}{4} j \delta (Z_e + Z_o) \text{sen } \vartheta \quad (4)$$

$$S_{31} \approx \frac{1}{4} j 2 (Z_e - Z_o) \text{sen } \vartheta \quad (5)$$

$$S_{41} \approx \frac{1}{4} j \delta (Z_e - Z_o) \text{sen } \vartheta \quad (6)$$

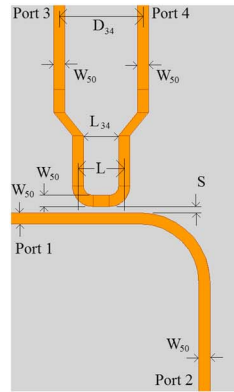
$$C = S_{31} \quad (7)$$

$$D = \frac{S_{31}}{S_{41}} \quad (8)$$

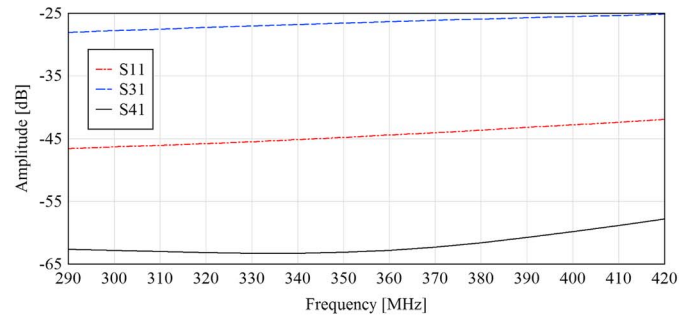
Since $\delta \ll 1$, (8) provides a high directivity D , as expected.

Let us consider the coupled line directional coupler shown in Figure 8: W_C is the width of the coupled microstrip lines, L_C is the length of the lines, and S_C is the spacing between them.

For the sake of simplicity we set $W_C = W_{50}$, W_{50} being the width of a 50 Ω isolated microstrip line using the Arlon AD1000 substrate, 3.2258 mm thick, with an equivalent value of the dielectric permittivity of 12.5, as characterized for operation at the temperature of 20 K. At this point, we can fix S_C , which determines Z_e and Z_o [Wadel, 1991] and, using (5), we can compute L_C to obtain the required -26 dB coupling. Then, if we choose $S_C = 1.35$ mm, which corresponds to $Z_e = 1.26$ and $Z_o = 0.72$ (i.e., $\delta = 0.093$), we derive $\vartheta = 10.15^\circ$ (i.e., $L_C = 8.45$ mm). In this case (4) gives $S_{11} = -41$ dB and (6) gives $S_{41} = -52$ dB. As predicted, a coupled line



(a)



(b)

Figure 9. Geometry and simulated (Ansys HFSS) scattering parameters of the directional coupler. The spacing $D_{34} = 18$ mm between ports 3 and 4 and the bend toward port 2 are constrained by the housing of the component inside the cryostat. The other geometrical parameters are $W_{50} = 2.43$ mm, $L_{34} = 7.5$ mm, and $L = L_{34} + W_0 = 9.93$ mm.

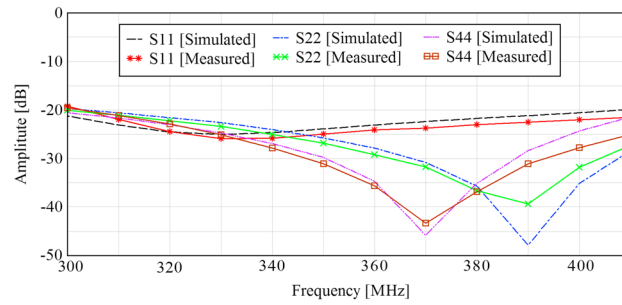


Figure 10. Reflection coefficients (S_{11} , S_{22} , and S_{44}) for the device in Figure 7.

speaking, the design equation (5) cannot be used to design this component since it does not account for the 90° bends at the ports 3 and 4. However, we can set the spacing S equal to S_C and equation (5) can be used as a first approximation, leading to $L = L_C$. Then, the directional coupler of Figure 9a with $S = S_C (=1.35 \text{ mm})$ and $L = L_C (=8.45 \text{ mm})$ has been simulated using Ansys HFSS, and we have found that the coupling S_{31} at the center frequency is -28 dB . In order to achieve the required coupling of -26 dB , L should be increased (5), and, using a simple HFSS parametric sweep, we have found the final value of L , which is equal to 9.93 mm .

The simulated scattering parameters $|S_{11}|$, $|S_{31}|$, and $|S_{41}|$ of the designed directional coupler in Figure 9a are reported in Figure 9b, whereas the simulated insertion loss $|S_{21}|$ is between 0.037 dB and 0.051 dB over the operating frequencies (300–410 MHz). As required, the simulated coupling coefficient at the center frequency of 355 MHz is -26 dB and the simulated directivity is larger than 30 dB .

3.2. Test of the Full Device at Cryogenic Temperature

The directional coupler proposed in section 3.1 is cascaded to the optimized fractal hybrid presented in section 2, which has been suitably rescaled, based on the properties of the Arlon AD1000 substrate at the temperature of 20 K . The resulting device is shown in Figure 7. This component has been realized in the laboratories of the Astronomical Observatory of Cagliari and tested at cryogenic temperature (20 K).

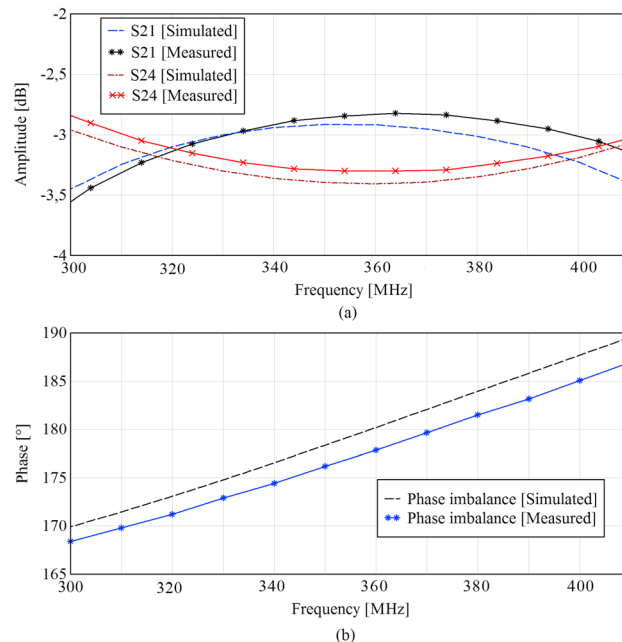


Figure 11. Frequency response of for the device in Figure 7: (a) Transmission coefficients (S_{21} and S_{24}) and (b) phase imbalance.

directional coupler with small electrical length can be used to achieve weak coupling, high return loss, and a directivity larger than 20 dB , as required by our radio astronomy application.

The position of the ports of the directional coupler to be employed in the P-band cryogenic receiver of SRT is dictated by the housing of the component inside the cryostat (Figure 7). As a result of this constraint the configuration shown in Figure 9a is adopted. Strictly

In Figure 10 the reflection at ports 1, 2, and 4 is reported, in Figure 11 the transmission coefficients S_{21} and S_{24} and the phase unbalance are shown, and in Figure 12 the coupling S_{26} and the isolation S_{25} are depicted. The agreement between simulation and measurement is good, with measured reflection below -19 dB (simulated below -20 dB), measured phase imbalance between 169° and 189° (simulated between 170° and 190°), and measured amplitude imbalance of 0.75 dB (simulated 0.5 dB). The measured coupling S_{26} is stable over the $300\text{--}410 \text{ MHz}$ frequency range (between -26.9 dB and -26.2 dB), and the isolation S_{25} is below -45 dB .

Finally, in Figure 13 the overall measured percentage power loss of the component is estimated by using the following

$$P_L = 1 - \sum_{i=1}^6 |S_{i2}|^2.$$

As apparent, the realized prototype exhibits very low losses at cryogenic temperature,

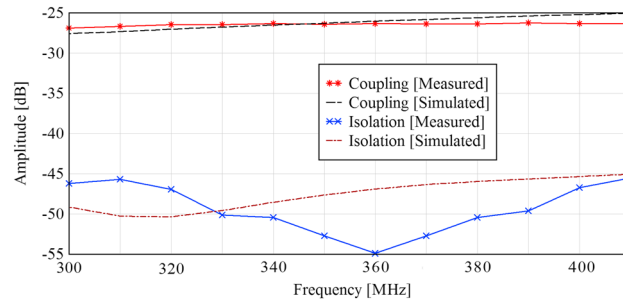


Figure 12. Coupling (S_{26}) and isolation (S_{25}) for the device in Figure 7.

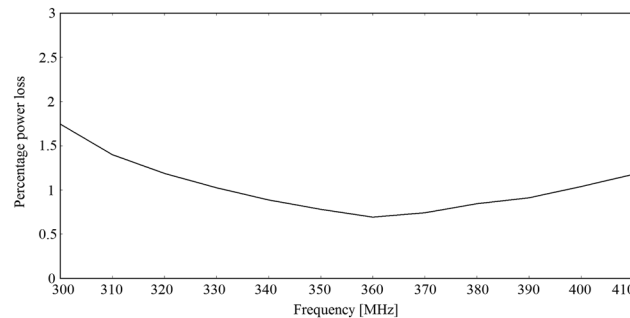


Figure 13. Percentage power loss of the component, when feeding from port 2.

i.e., less than 2% over the bandwidth, taking into account the losses of microstrip lines, connectors, through walls, and solderings.

4. Conclusions

A planar 180° fractal hybrid providing high return loss and a directional coupler with weak coupling and high isolation are proposed for radio astronomy applications, aiming to a compact, light, and reliable design. In particular, these components are intended to be used in the cryogenic receiver of the Sardinia Radio Telescope, operating between 300 MHz and 410 MHz, at the temperature of 20 K. Based on the 180° fractal hybrid proposed by Ghali, an optimization has been carried out to comply with the stringent requirements of the SRT P-band radio astronomy receiver. The optimized hybrid provides a bandwidth improvement over the standard configuration for both the return loss and the amplitude imbalance. The fractal 180° hybrid and the

directional coupler have been manufactured in the same layout and tested at the cryogenic temperature of 20 K, showing a return loss greater than 19 dB and an amplitude imbalance less than 0.75 dB over the operating frequency band.

Acknowledgments

The data supporting the conclusions of this work are listed in the tables and figures.

References

- Bolli, P., et al. (2015), Sardinia Radio Telescope: General description, technical commissioning and first light, *J. Astronom. Instrum.*, 4(4–5), 1–20, doi:10.1142/S2251171715500087.
- Chuang, M. L. (2005), Miniaturized ring coupler of arbitrary reduced size, *IEEE Microwave Wireless Components Lett.*, 15(1), 16–18, doi:10.1109/LMWC.2004.840960.
- Dydyk, M. (1999), Microstrip directional couplers with ideal performance via single-element compensation, *IEEE Trans. Microwave Theory Tech.*, 47(6), 956–964, doi:10.1109/22.769332.
- Eccleston, K. W. (2003), Compact planar microstripline branch-line and rat-race couplers, *IEEE Trans. Microwave Theory Tech.*, 51(10), 2119–2125, doi:10.1109/TMTT.2003.817442.
- Fano, R. M. (1947), Theoretical limitations on the broadband matching of arbitrary impedances, *Tech. Rep. 41*, Mass. Inst. of Technol., Res. Lab. of Electr.
- Foster, R. M. (1924), A reactance theorem, *Bell Syst. Tech. J.*, 3(2), 259–267, doi:10.1002/j.1538-7305.1924.tb01358.x.
- Ghali, H., and T. A. Moselhy (2004), Miniaturized fractal rat-race, Branch-line, and coupled-line hybrids, *IEEE Trans. Microwave Theory Tech.*, 52(11), 2513–2520, doi:10.1109/TMTT.2004.837154.
- Iwer, H. W. (1980), Quarter wave microstrip directional coupler having improved directivity, United States Patent 4216446, August 1980.
- Kerr, A. R. (2001), 'Elements for E-Plane Split Blocks Waveguide Circuits' in *ALMA Memo n. 381*, pp. 1–9, Natl. Radio Astron.Obs., Charlottesville, Va.
- Kim, C. S., J. S. Lim, D. J. Kim, and D. Ahn (2004), A design of single and multi-section microstrip directional coupler with high directivity, *IEEE MTT-S Int. Microwave Symp. Dig.*, 3, 1895–1898, doi:10.1109/MWSYM.2004.1338978.
- Liu, H., S. Fang, Z. Wang, and S. Fu (2014), Novel coupled line 180 hybrid with non-interspersed input and output ports, *IEEE Trans. Microwave Theory Tech.*, 62(11), 2641–2649, doi:10.1109/TMTT.2014.2356977.
- Mo, T. T., Q. Xue, and C. H. Chan (2007), A broadband compact microstrip rat-race hybrid using a novel CPW inverter, *IEEE Trans. Microwave Theory Tech.*, 55(1), 161–166, doi:10.1109/TMTT.2006.888938.
- Napijalo, V. (2012), Coupled line 180 hybrids with large couplers, *IEEE Trans. Microwave Theory Tech.*, 60(12), 3674–3682, doi:10.1109/TMTT.2012.2217980.
- Nedlin, G. (1989), Energy in lossless and low-loss networks, and Foster's reactance theorem, *IEEE Trans. Circuits Syst.*, 36(4), 561–567, doi:10.1109/31.92888.
- Okabe, H., C. Caloz, and T. Itoh (2004), A compact enhanced-bandwidth hybrid ring using an artificial lumped-element left-handed transmission-line section, *IEEE Trans. Microwave Theory Tech.*, 52(3), 798–804, doi:10.1109/TMTT.2004.823541.
- Pozar, D. M. (2012), *Microwave Engineering*, 4th ed., pp. 317–379, Wiley, Hoboken, N. J.

- Settaluri, R. K., G. Sundberg, A. Weisshaar, and V. K. Tripathi (2000), Compact folded line rat-race hybrid couplers, *IEEE Microwave Guided Wave Lett.*, *10*(2), 61–63, doi:10.1109/75.843101.
- Simion, S., and G. Bartolucci (2014), Broadband and small-size 3-dB ring coupler, *Progr. Electromagn. Res. Lett.*, *44*, 23–28, doi:10.2528/PIERL13101001.
- Valente, G., G. Montisci, and S. Mariotti (2014), High-performance microstrip directional coupler for radio-astronomical receivers at cryogenic temperature, *Electron. Lett.*, *50*, 449–451, doi:10.1049/el.2014.0078.
- Valente, G., G. Montisci, T. Pisanu, A. Navarrini, P. Marongiu, and G. A. Casula (2015), A compact L-band orthomode transducer for radio astronomical receivers at cryogenic temperature, *IEEE Trans. Microwave Theory Tech.*, *63*(10), 3218–3227, doi:10.1109/TMTT.2015.2464809.
- Wadel, B. C. (1991), *Transmission Line Design Handbook*, 1st ed., pp. 181–377, Artech House, Norwood, Mass.
- Wang, C., and K. A. Zaki (1996), Full-wave modeling of generalized double ridge waveguide T-junctions, *IEEE Trans. Microwave Theory Tech.*, *44*(12), 2536–2543, doi:10.1109/22.554596.
- Yang, N., C. Caloz, and K. Wu (2010), Broadband compact 180 hybrid derived from the Wilkinson divider, *IEEE Trans. Microwave Theory Tech.*, *58*(4), 1030–1037, doi:10.1109/TMTT.2010.2042631.